Layout and Experimental Results of an 10/40 kW rSOC Demonstration System

Ro. Peters[a], N. Kruse[a], W. Tiedemann[a], I. Hoven[a], R. Deja[a], D. Schäfer[a], F. Kunz[a], and R.-A. Eichel[a,b]

[a] Forschungszentrum Jülich GmbH, Institute of Energy and Climate Research (IEK-9), 52428 Jülich, Germany
[b] RWTH Aachen University, Institute of Physical Chemistry, Templergraben 55, 52074 Aachen, Germany

Forschungszentrum Jülich has been operating an rSOC system in the 10/40 kW_{AC} power class since 2021. This system uses four 20-layer sub-stacks in the mark H20 stack design. During the test campaign, a power range from 1.7 to 13 kW_{AC} could be shown in fuel cell mode. The highest efficiency in fuel cell mode of 63.3 % was achieved at a power output of 10.4 kW_{AC}, related to the lower heating value (LHV) of hydrogen. With a power input of -49.6 kW_{AC}, the highest efficiency of 71.1 % (LHV) was achieved in electrolysis mode. At this point, 11.7 $Nm^3\ h^{-1}$ of hydrogen were produced. The following manuscript shows the layout and the experimental results of the rSOC demonstration system.

Introduction

Within the last years, the development work on reversible solid oxide cell (rSOC) systems has been intensified. Because this technology can contribute to a carbon-neutral energy supply by storing electrical power into hydrogen in times when the supply of renewably produced electricity in the grid is greater than the demand and reconverting it into electrical power vice versa. In the following, results from the operation of different rSOC demonstration systems are reported. A system from the Technical Research Center of Finland (VTT) achieved a system efficiency in electrolysis mode of 60 % based on the lower heating value (LHV) of hydrogen in the context of the EU project BALANCE at a current density of $-630\ mA\ cm^{-2}$ and 750 °C (1). Furthermore, the company Sunfire presented a system from the GrInHy project, which consists of 48 stacks, each with 30 cells and a maximum power of 143 kW. The efficiency in fuel cell mode is 48 % (LHV) and in electrolysis mode 84 % (LHV) (2). The University Grenoble Alpes (CEA) showed results of a 4.8 kW demonstration system which could operate at a steam utilization of 95 % at an operating temperature of 800 °C. It could be shown that the switching times between the fuel cell and electrolysis operations are between 8 and 10 minutes (3). In a thermodynamic analysis, Forschungszentrum Jülich showed that a round trip efficiency of 50 % is possible for a pressurized storage at 70 bar (4). Encouraged by this result, an rSOC demonstration system whose design point is 5 kW_{DC} in fuel cell mode and 15 kW_{DC} in electrolysis mode was developed (5, 6). This system was able to achieve more than 62 % efficiency in fuel cell mode and 70 % in electrolysis mode, both based on LHV and DC power. In a next step, a second rSOC system was developed and tested, in which the system performance was significantly increased in fuel cell and electrolysis mode.

Experimental Setup, Results and Discussion

The main component of the system is the Integrated Module (IM), whose components are shown in Figure 1. It consists of four 20-layer sub-stacks in the mark H20-design with an active cell area of 320 cm² developed by Forschungszentrum Jülich. The fuel and air heaters are located at the very top and bottom of the IM. The system can be heated up from room to operation temperature by five heating plates which are arranged on top and below each sub-stack. These plates are also used to provide heat to the stacks during the endothermic electrolysis operation. The overall dimensions of the IM are length x width x height : 0.399 m x 0.224 m x 0.973 m. In operation, the IM is covered with 0.1 m thick microporous thermal insulation at all sides.

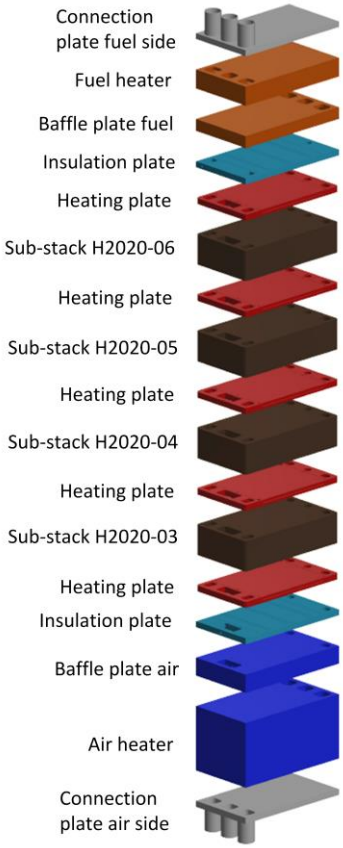

Figure 1. CAD drawing of the Integrated Module including sub-stacks, heating plates, air an fuel heaters as well as additional components used in the rSOC demonstration system, reproduced from (7).

In addition to the IM, all necessary balance of plant (BoP) components, the media supply, the control and safety systems are connected as shown in Figure 2. The system described here is equipped with a recirculation unit, which returns part of the fuel side off-gas of the IM back to its inlet. The steam contained in the recirculated gas stream will be largely condensed bevor entering the diaphragm compressor. With the help of the recirculation unit and the steam condensation, a system fuel utilization (Fu_{System}) of almost 100% can be achieved during the fuel cell mode.

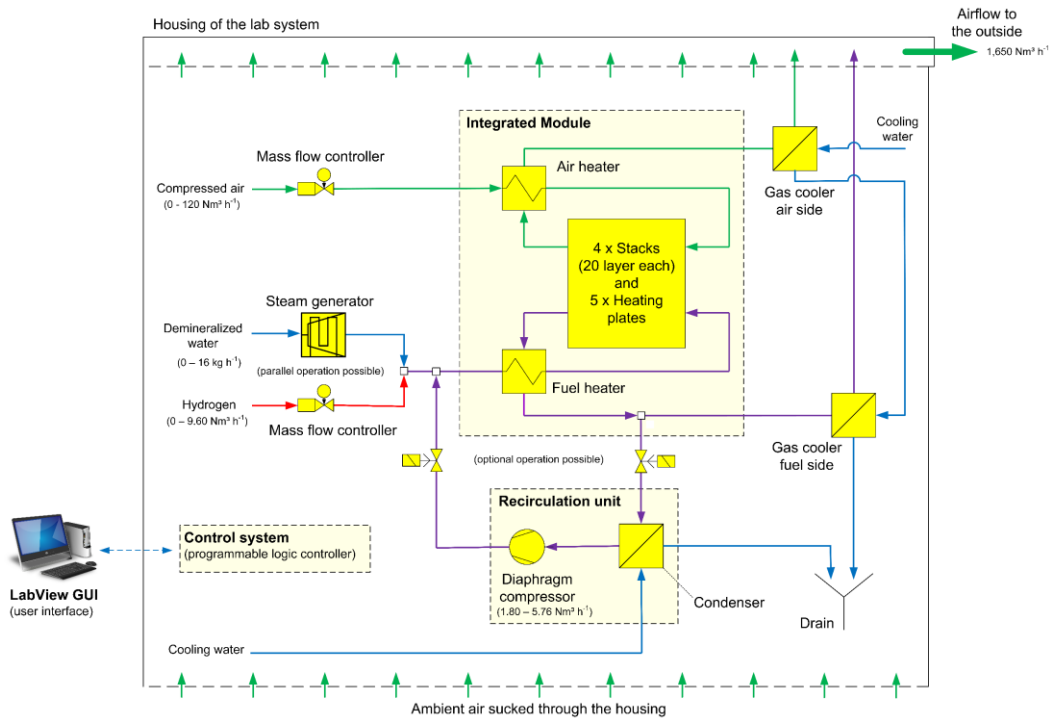

Figure 2. Simplified flow scheme of the rSOC demonstration system including the Integrated Module, the recirculation unit and necessary balance of plant components for the system operation, reproduced from (7).

The system was set into operation in a laboratory of the Forschungszentrum Jülich for the first time on June 01, 2021. The integration of the test setup is depicted in Figure 3.

Figure 3. Test environment of the system in the laboratory. The white rectangular block the center of the picture is the thermally insulated Integrated Module.

The system operation started with stationary operating points in fuel cell and electrolysis mode. The performance, efficiency and temperature data achieved during the operating phase are shown below.

Experimental Result of Fuel Cell Mode

The electrical efficiency of the fuel cell operation was calculated according to equation 1. It must be mentioned that the system is operated with an electronic load instead of an inverter. Therefore, a constant DC/AC inverter efficiency of 0.95 is assumed here.

$$\eta_{Fuel\ cell,AC} = \frac{Power\ output\ (AC)}{H2\ input\ (LHV)} = \frac{U_{Stack} \cdot I_{Stack} \cdot \eta_{Inverter} - \sum P_{BoP,AC}}{\dot{n}_{H2,\,system\ in} \cdot LHV_{H2}} \quad [1]$$

$\eta_{Fuel\ cell,\,AC}$	System efficiency in fuel cell mode
U_{Stack}	Stack voltage
I_{Stack}	Stack curent
$\eta_{Inverter}$	DC/AC inverter efficiency (assumed to be 0.95)
$\sum P_{BoP}$	Consumption of BoP components
$\dot{n}_{H2,\,system\ in}$	Molar flow of hydrogen at the inlet of the system
LHV_{H2}	Lower heating value of hydrogen

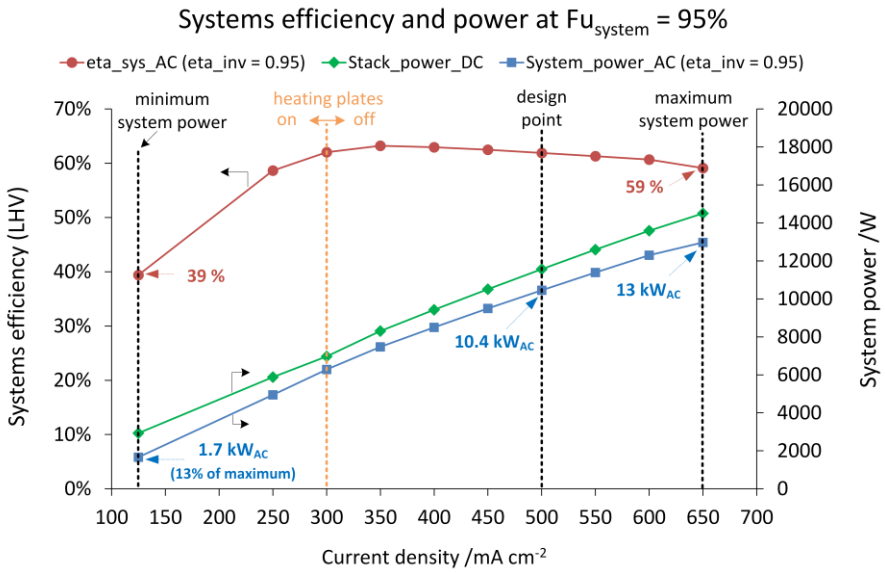

Figure 4. Performance characteristics and efficiency of the system in fuel cell mode for a fuel utilization of 95 % while varying the current density.

Figure 4 shows the performance characteristics in fuel cell mode for a system fuel utilization of 95%, with a variation of the current density from 125 to 650 mA cm^{-2}. The design point of the system is 500 mA cm^{-2}. At this point, a power output of 10.4 kW$_{AC}$ could be achieved. The current density variation mentioned above corresponds to a power

range of 1.7 to 13kWAC (blue line). The minimum excess air ratio is reached at 350 mA cm^{-2}, which is why the heating plates must be activated below this current density to prevent the stacks from cooling down. A system efficiency (red line) of 59 % is achieved at a current density of 650 mA cm^{-2}. A strong drop in efficiency can be seen, when the current density is reduced below 350 mA cm^{-2}, because the heating plates are activated and causing a higher consumption of the BoP. However, at the minimum current density of 125 mA cm^{-2}, a efficiency of 39 % is still achieved.

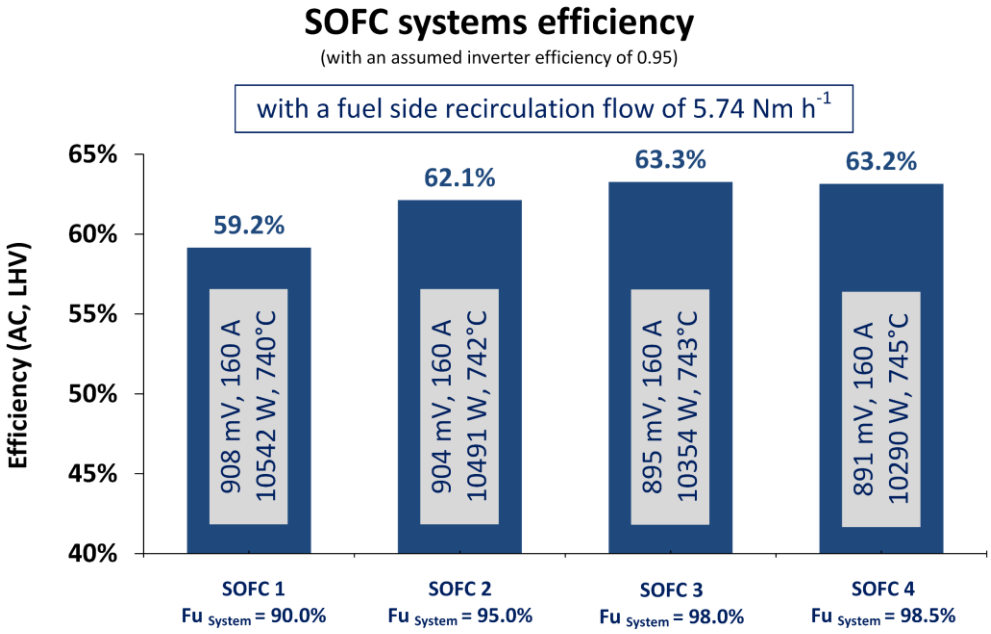

Figure 5. System efficiency in fuel cell mode with variation of the system fuel utilization for a constant current density of 500 ma cm^{-2}.

Figure 5 shows the electrical system efficiencies when varying the system fuel utilization for a constant current density of 500 mA cm^{-2} at a recirculation flow rate of 5.74 Nm^3 h^{-1} (at 0°C, 1.013bar). For case SOFC 1, an average cell voltage of 908 mV could be achieved with a system fuel utilization of 90.1 %. These results in an electrical system efficiency of 59.2 % and an AC power output of 10542 W. In case SOFC 2, system fuel utilization has been raised to 95.0 %. Here the cell voltage drops by 4 mV and the stack power by 51 W, but the system efficiency increases to 62.1 %, due to the lower hydrogen input to the system. With SOFC 3, the fuel efficiency is further increased to 98.0 % while the cell voltage is reduced to 895 mV, resulting in a power reduction to 10354 W. Again, the lower hydrogen supply increases efficiency up to 63.3 %. For SOFC 4, the fuel utilization has been increased to 98.5 %. The cell voltage and the stack power fell slightly again, but here the system efficiency also fell to 63.2 %. For this case, the positive effect by reducing the hydrogen was overcompensated by the higher power consumption of the air compressor.

Figure 6 shows a CAD drawing of the IM in a non-exploded view. The blue circles mark the thermocouple positions to measure the temperature distribution in the cell area of the four stacks.

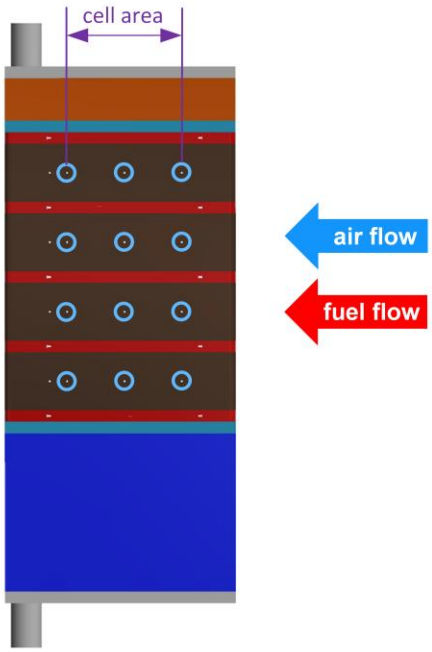

Figure 6. CAD drawing of the Integrated Module in a non-exploded view. The blue circles mark the thermocouple positions in the cell area of the stack.

The result for the case SOFC 3 is shown in Figure 7. The gas inlet side shows the lowest temperatures, due to the coflow design of the stacks. By the heat released from the electrochemical reaction the temperatures will rise towards the gas outlet. Therefore, the temperature gradient over the cell area is about 140 °C. The outer stacks, here H2020-03 and H2020-06 (see Figure 1) show slightly lower temperatures than H2020-05 and H2020-04 in the middle of the IM. Because these stacks are adjacent to fuel and air heater, and a part of heat generated in the stacks is transferred to them.

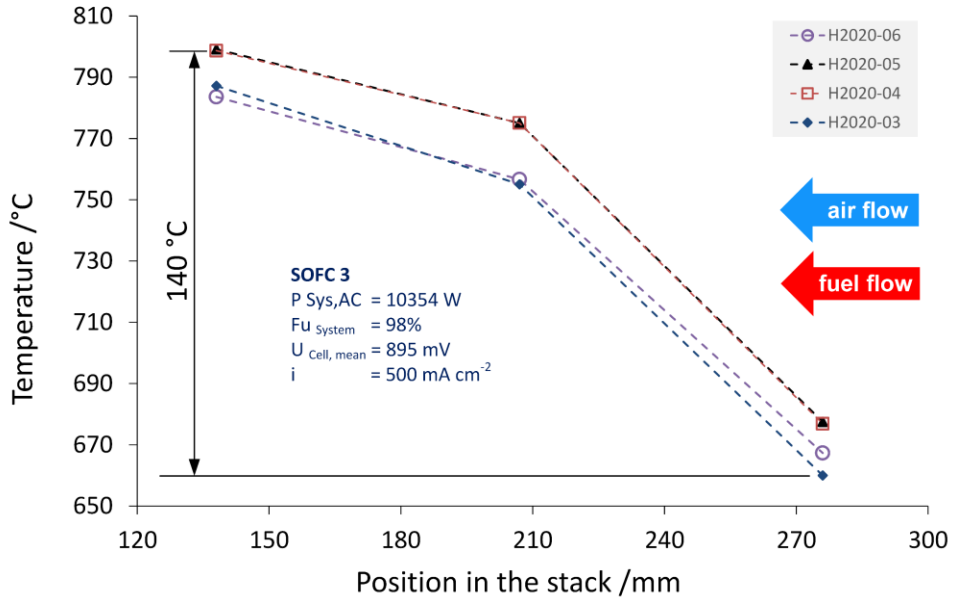

Figure 7. Temperature distribution in fuel cell mode for case SOFC 3 of the four sub stacks.

Experimental Results in Electrolysis Mode

The electrical efficiency of electrolysis mode is calculated by equation 2. Again, the laboratory system was operated with electronic power supplies and an AC/DC rectifier efficiency of 0.95 is assumed for the calculations.

$$\eta_{Electrolysis,AC} = \frac{H2\ output\ (LHV)}{Power\ input\ (AC)} = \frac{\dot{n}_{H2,\,produced} \cdot LHV_{H2}}{\frac{U_{Stack} \cdot I_{Stack}}{\eta_{Rectifier}} + \sum P_{BoP,\,AC}} \quad [2]$$

$\eta_{Electrolysis,AC}$	System efficiency in electrolysis mode
$\dot{n}_{H2,\,produced}$	Molar flow of hydrogen produced by the electrochemical reaction
$\eta_{Rectifier}$	AC/DC rectifier efficiency (assumed to be 0.95)

In total three operating points different steam utilizations (Su $_{System}$) were investigated at a constant current density – 1100 mA cm^{-2}, which corresponds to a hydrogen production rate of 11.7 Nm^3 h^{-1}. During the test procedure, a hydrogen content of 20 % is added to the steam at the fuel gas side. An external air flow is supplied on the air side of the stacks, which limits the oxygen content at the stack outlet to 50 %. The results are shown in Figure 8.

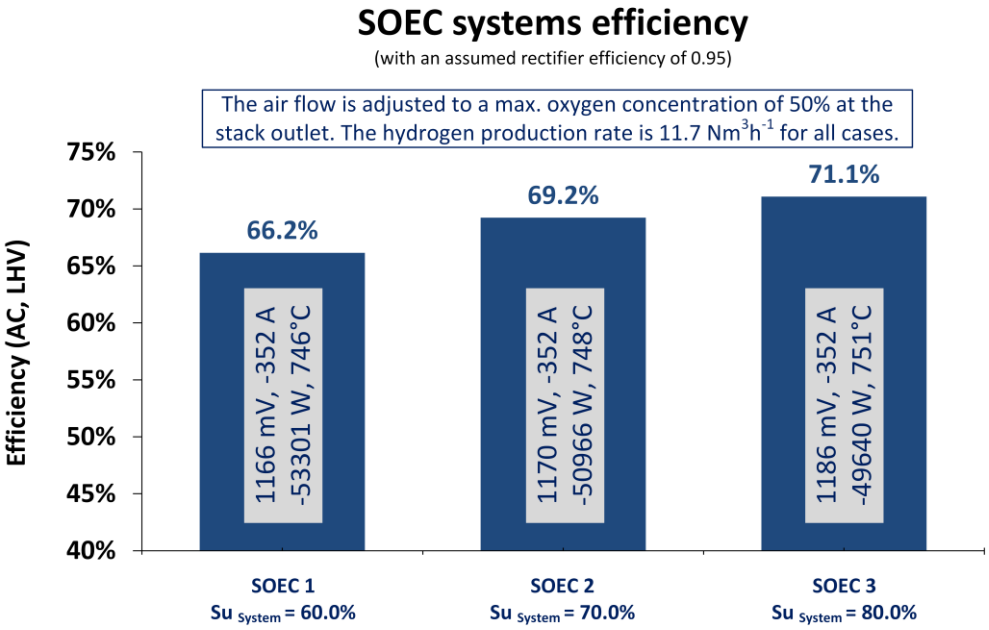

Figure 8. System efficiencies in electrolysis mode for a constant current density of -1100 mA cm^{-2} with a steam utilization variation from 60 to 80 %.

For case SOEC 1 with a steam utilization of 60 % a system efficiency of 66.2 % is reached at a cell voltage of 1166 mV and a corresponding system power input of -53301 W. For the operating case SOEC 2, the steam utilization was increased to 70 % and here the input power decreased to – 50966 W. In this case, less power had to be given to the steam

generator at the same hydrogen production rate, which reduces the BoP consumption significantly. Therefore, the system efficiency increases 69.2 %. A similar effect happens for case SOEC 3. Here, the steam utilization was further increased to 80 % and again due to the lower power input to the steam generator the efficiency increases to 71.1 %. These results reveal that the system efficiency in electrolysis strongly depends on the steam utilization, at least when the steam must be generated electrically.

The stack temperature distribution for case SOEC 3 is shown in Figure 9. Comparing the stack temperatures in fuel cell mode (see Figure 7) with the electrolysis mode, it is obvious that during the electrolysis operation the temperatures are more homogeneous. This behavior can be explained by the activated electrical heating plates. Because of the combination of temperature and cell resistance, all three operation cases in electrolysis mode, are operated with cell voltages below the thermoneutral voltage and therefore external heat must be supplied via the heating plates. Because of this effect, the heating plates prevent the temperature drop of the outer stacks towards the neighboring components. In addition to that, the air flow to the stack is significant lower in electrolysis mode, compare to the fuel cell operation, which is why the temperature gradient is only 75 °C, instead of 140 °C.

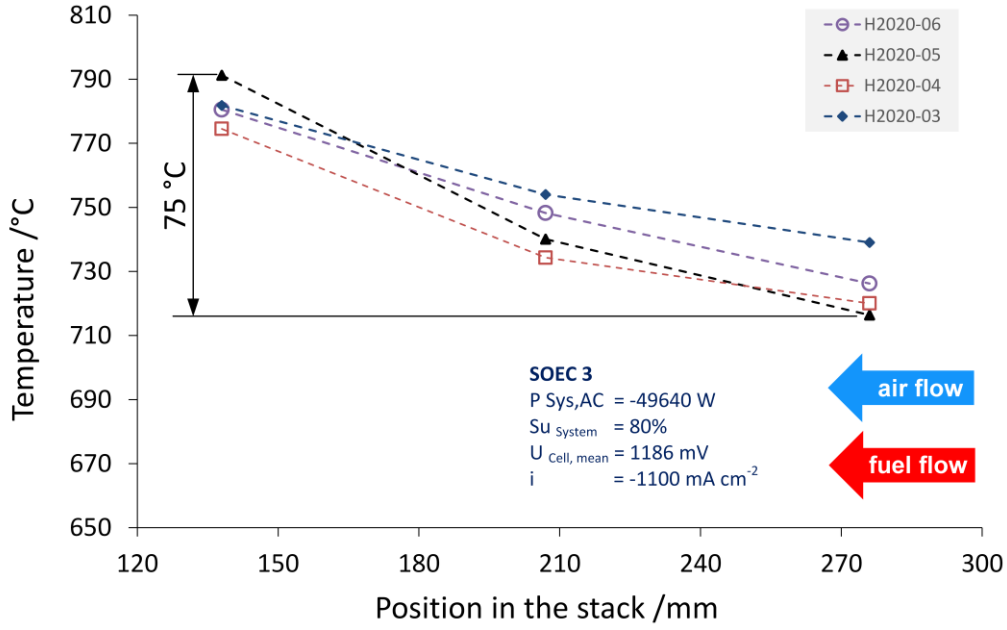

Figure 9. Temperature distribution in electrolysis mode for case SOEC 3 of the four sub stacks.

Conclusion and Outlook

The layout and the experimental results of a 10/40 kW-class rSOC system at Forschungszentrum Jülich has been shown. The system can be operated in fuel cell mode in a power range from 1.7 kW_{AC} at 125 mA cm^{-2} to 13 kW_{AC} at 650 mA cm^{-2}. A maximum electrical system efficiency of 63.3 % at a system power output of 10.4kW_{AC} and a fuel utilization of 98 % could be shown. This high level of efficiency was achieved through a

low cell resistance, the use of a recirculation unit including steam condensation and a low system pressure loss of the system and thus a low BoP consumption. During operation, a temperature gradient of 140°C was measured in the cell area of the stacks. It could also be observed that the outer sub-stacks have a lower temperature because they transfer heat to the neighboring components.

During the electrolysis mode, an efficiency of 71.1 % for a current density of - 100 mA cm^{-2} at a corresponding input power of - 49.6 kW with a steam utilization of 80 % was achieved. At this operating point, the temperature gradient in the cell area of the stacks is with 75 °C more homogeneous compared to fuel cell mode.

In future work new methods of stack temperature control based on artificial neural networks will be investigated on basis of the presented system. Afterwards it is planned to apply realistic load profiles to the system while investigating the performance, temperature, and degradation behavior. Furthermore, electricity and gas storage as well as heat decoupling for district heating application will be studied.

Acknowledgments

The authors would like to thank their colleagues at Forschungszentrum Jülich GmbH for their great support and the Helmholtz Society, the German Federal Ministry of Education and Research as well as the Ministry of Culture and Science of the Federal State of North Rhine-Westphalia for financing these activities as part of the Living Lab Energy Campus. In particular, we would like to thank Mr. Rabah Lekehal and Mr. Stefan Küpper for their help in setting up and operating the demonstration system.

References

1. V. Saarinen, J. Pennanen, M. Kotisaari, O. Thomann, O. Himanen, S. D. Iorio, P. Hanoux, J. Aicart, K. Couturier, X. Sun, M. Chen and B. R. Sudireddy, *Fuel Cells*, **21**, 477 (2021).
2. O. Posdziech, K. Schwarze and J. Brabandt, *International Journal of Hydrogen Energy* (2018).
3. J. Aicart, S. Di Iorio, M. Petitjean, P. Giroud, G. Palcoux and J. Mougin, *Fuel Cells*, **19**, 381 (2019).
4. M. Frank, R. Deja, R. Peters, L. Blum and D. Stolten, *Applied Energy*, **217**, 101 (2018).
5. R. Peters, M. Frank, W. Tiedemann, I. Hoven, R. Deja, V. N. Nguyen, L. Blum and D. Stolten, *ECS Transactions*, **91**, 2495 (2019).
6. R. Peters, M. Frank, W. Tiedemann, I. Hoven, R. Deja, N. Kruse, Q. Fang, L. Blum and R. Peters, *Journal of the Electrochemical Society* (2021).
7. R. Peters, W. Tiedemann, I. Hoven, R. Deja, N. Kruse, Q. Fang, L. Blum and R. Peters, *ECS Transactions*, **103**, 289 (2021).